J. Comput. Assist. Tomogr. **115**, 565 (1992)] between the individual MRIs and the atlas, the median brain among the population of participants was labeled as typical. Smoothed, normalized PET data were analyzed with the use of SPM software with a multisubject block design, two replications per condition, and an analysis of covariance global normalization. Participant and global brain activity were two covariates of no interest, and the conditions of the task were the covariates of interest. The search volume was from $z = -30$ mm to $z = 60$ mm and did not allow a complete view of the cerebellum. In the parametric test, the contrasts represented the average movement length per condition. In the subtraction tests, the contrasts were −1 and 1 (or 1 and −1) for the conditions of interest. We considered as significant regions where voxel-level Z values exceeded 4.4 so that the corrected $P < 0.05$. We also considered as significant regions in the sensorimotor system that we had selected a priori, where voxel-level Z values exceeded 3.09. These regions were the primary sensorimotor, the premotor, and the supplementary motor areas, the striatum, and the cerebellum.

19. C. Dettmers *et al.*, *J. Neurophysiol.* **74**, 802 (1995).
20. Principal component analysis [K. J. Friston, C. D. Frith, R. S. J. Frackowiak, *Proc. R. Soc. London Ser. B* **254**, 47 (1993)] of the data in session 1 showed that changes in rCBF in regions of the left BA 18, thalamus, and right BA 46 were highly correlated. The images from each participant were projected through the eigenimage that represented this network. The result was a score that was minimum in the random field condition and maximum during early learning. This suggests that the network was least active when the task was most novel (participants experienced a field for the first time in the random condition) yet unlearnable, and was most active only when the task was being rapidly learned. Therefore, it is likely that the increase in BA 46 (Fig. 2B) in early learning versus the random condition is learning-related and not due to confounding factors such as the novelty or attention requirements of the task.
21. G. S. Brindley, *Int. Brain Res. Org. Bull.* **3**, 80 (1964); J. M. Fuster, *Memory in the Cerebral Cortex: An Empirical Approach to Neural Networks in the Human and Nonhuman Primates* (MIT Press, Cambridge, MA, 1995); W. T. Thach, *Behav. Brain Sci.* **19**, 411 (1996).
22. A. Pascual-Leone, E. M. Wassermann, J. Grafman, M. Hallett, *Exp. Brain Res.* **107**, 479 (1996).
23. Previous experiments (*8*) suggest that after 400 targets in a field, up to 50% further practice during session 1 does not result in significantly improved performance.
24. S. Grafton *et al.*, *J. Neurosci.* **12**, 2542 (1992); K. J. Friston, C. D. Frith, R. E. Passingham, P. F. Liddle, R. S. Frackowiak, *Proc. R. Soc. London Ser. B* **248**, 223 (1992); D. M. Clower *et al.*, *Nature* **383**, 618 (1996).
25. R. J. Seitz, P. E. Roland, C. Bohm, T. Greitz, S. Stone-Elander, *Neuroreport* **1**, 57 (1990); I. H. Jenkins, D. J. Brooks, P. D. Nixon, R. S. J. Frackowiak, R. E. Passingham, *J. Neurosci.* **14**, 3775 (1994).
26. M. Jueptner *et al.*, *J. Neurophysiol.* **77**, 1313 (1997).
27. J. Quintana and J. M. Fuster, *Neuroreport* **3**, 721 (1992); W. W. Shindy, K. A. Posley, J. M. Fuster, *Cereb. Cortex* **4**, 443 (1994).
28. P. S. Goldman-Rakic, *Proc. Natl. Acad. Sci. U.S.A.* **93**, 13473 (1996).
29. D. Marr, *J. Physiol. London* **202**, 437 (1969); J. S. Albus, *Math. Biosci.* **10**, 25 (1971); M. Ito, *Brain Res.* **40**, 80 (1972); K. Sasaki and H. Gemba, *Exp. Brain Res.* **48**, 429 (1982); M. Kawato and H. Gomi, *Biol. Cybern.* **68**, 95 (1992); M. Shidara, K. Kawano, H. Gomi, M. Kawato, *Nature* **365**, 50 (1993); J. C. Houk and S. P. Wise, *Cereb. Cortex* **5**, 95 (1995); J. L. Raymond, S. G. Lisberger, M. D. Mauk, *Science* **272**, 1126 (1996); J. A. Kleim, K. Vij, D. H. Ballard, W. T. Greenough, *J. Neurosci.* **17**, 717 (1997).
30. R. Shadmehr and K. A. Thoroughman, in *Neuro-Mechanical Interaction in Posture and Movement Control*, J. Winters and P. Crago, Eds. (Springer-Verlag, New York, in press).
31. H. P. Goodkin, J. G. Keating, T. A. Martin, W. T. Thach, *Can. J. Neurol. Sci.* **20**, S93 (1993); A. J. Bastian, T. A. Martin, J. G. Keating, W. T. Thach, *J. Neurophysiol.* **76**, 492 (1996).
32. C. L. Ojakangas and T. J. Ebner, *J. Neurophysiol.* **68**, 2222 (1992).
33. N. W. Seeds, B. L. Williams, P. C. Bickford, *Science* **270**, 1992 (1995).
34. K. Sasaki and H. Gemba, *Brain Res.* **374**, 278 (1986); R. E. Passingham, *Exp. Brain Res.* **70**, 590 (1988); *Brain Behav. Evol.* **33**, 189 (1989); U. Halsband and H.-J. Freund, *Brain* **113**, 207 (1990); L. Germain and Y. Lamarre, *Brain Res.* **611**, 175 (1993); Y.-C. Chen, D. Thaler, P. D. Nixon, C. E. Stern, R. E. Passingham, *Exp. Brain Res.* **102**, 461 (1995).
35. A. R. Mitz, M. Godschalk, S. P. Wise, *J. Neurosci.* **11**, 1855 (1991); D. Boussaoud and S. P. Wise, *Exp. Brain Res.* **95**, 28 (1993).
36. S. P. Wise, in *The Acquisition of Motor Behavior in Vertebrates*, J. R. Bloedel, T. J. Ebner, S. P. Wise, Eds. (MIT Press, Cambridge, MA, 1996), pp. 261–286.
37. J. Tanne, D. Boussaoud, N. Boyer-Zeller, E. M. Rouiller, *Neuroreport* **7**, 267 (1995).
38. P. B. Johnson, S. Ferraina, L. Bianchi, R. Caminiti, *Cereb. Cortex* **6**, 102 (1996).
39. H. Poizner *et al.*, *Brain* **118**, 227 (1995); A. Sirigu *et al.*, *Science* **273**, 1564 (1996).
40. We thank K. Akhavan-Toyserkani, Z. Zhao, K. Thoroughman, M. Smith, B. S. Yu, S. Wise, and the scientists at the Johns Hopkins PET facility, led by R. Dannals. This work was funded in part by the Whitaker Foundation, the National Institute of Mental Health, and the Office of Naval Research.

24 February 1997; accepted 24 June 1997

Drosophila Mitotic Domain Boundaries as Cell Fate Boundaries

Sidney B. Cambridge, Robert L. Davis, Jonathan S. Minden*

Fate determination in *Drosophila* embryos is evidenced by the appearance of mitotic domains. To identify fate or fates of cells, individual cells in mitotic domains 2, 8, and 15 were marked and monitored through development. Comparison of the different fates indicated that domain boundaries are cell fate boundaries. Cells were marked by expression of GAL4-dependent transgenes after photoactivation of a caged GAL4VP16 analog that had its DNA binding activity inhibited with a photolabile blocking reagent. Caged GAL4VP16 was also used to induce gene expression in *Xenopus* embryos. Thus, photoactivated gene expression is a versatile tool for spatiotemporal control of gene expression.

To control the temporal and spatial expression of selected genes at the single-cell level for the purpose of fate mapping and genetic manipulation, we devised a method for "caging" the DNA binding activity of GAL4VP16, a potent transcriptional activator. Caging is a form of photo-reversible chemical modification that has been used in the light-mediated activation of molecules such as adenosine 5′-triphosphate, Ca^{2+}-chelators, and actin (*1*). Caged GAL4VP16 was produced by modifying lysine residues of purified GAL4VP16 (*2*) with the amine-reactive compound 6-nitroveratrylchloroformate (NVOC-Cl) (*3*). GAL4VP16 DNA binding activity was abolished after a 30-min incubation with 2 mM NVOC-Cl under mildly basic conditions (Fig. 1A). More than 50% of the initial binding activity was recovered by irradiating the caged GAL4VP16 with a low-intensity, long-wavelength (365 nm) ultraviolet (UV) lamp.

Caging of GAL4VP16 with 0.5 mM NVOC-Cl, which modified about 8 of the 14 GAL4VP16 lysines (*4*), completely inhibited in vivo transcriptional activation in *Drosophila* embryos (*5*). This level of caging did not affect GAL4VP16 DNA binding activity in vitro (Fig. 1A). It is not known why the lower level of caging inhibited in vivo activity (*6*). Inhibition of the transcriptional activity of caged GAL4VP16 could be reversed in vivo with 365-nm light from a 100-W mercury lamp shone through a microscope objective via the epi-fluorescence light path of a standard inverted microscope. Experiments with *Drosophila* embryos required 3 to 4 s of irradiation (*7*) for maximal photoactivation.

We determined the efficiency of GAL4VP16-mediated photoactivated gene expression by quantitating the fluorescence of coinjected RGPEG (*8*), a fluorogenic β-galactosidase (β-Gal) substrate, in embryos that contained a GAL4-dependent *lacZ* construct (UAS_G*lacZ*) (Fig. 1B). GAL4VP16 was usually injected at a concentration of 0.2 mg/ml or less (*9*). Concentrations of unmodified or caged GAL4VP16 greater than 0.4 mg/ml caused developmental defects. This may have resulted from squelching, where general transcription factors bound to the acidic domain of unbound GAL4VP16 (*10*). Injection of RGPEG alone or with caged GAL4VP16, but not followed by irradiation,

S. B. Cambridge and J. S. Minden, Department of Biological Sciences and Center for Light Microscope Imaging and Biotechnology, Carnegie Mellon University, Pittsburgh, PA 15213, USA.
R. L. Davis, Department of Cell Biology, Harvard Medical School, Boston, MA 02115, USA.

*To whom correspondence should be addressed. E-mail: minden@andrew.cmu.edu

gave curves that initially decreased to a constant, low level of fluorescence. This decrease may have been due to quenching of the fluorescence of trace-free resorufin in the RGPEG preparation by free thiols in the embryo such as glutathione (*11*). Irradiation of control embryos injected with RGPEG alone did not cause any increase in fluorescence (*12*). Injection of unmodified GAL4VP16 showed a marked increase in RGPEG fluorescence, indicating the induction of *lacZ* expression. Irradiation of embryos after injection of caged GAL4VP16 gave a response that was 74% of the unmodified GAL4VP16. Caged GAL4VP16 was photoactivated as early as nuclear cycle 12 and up to 4 hours after gastrulation at 25°C (*12*). Most of the irradiated embryos developed into normal stage 17 embryos. Whole-embryo irradiation did not alter cell death patterns as seen by time-lapse fluorescence microscopy of embryos coinjected with acridine orange to monitor apoptosis (*13*) and either GAL4VP16 or buffer (*12*).

To photoactivate gene expression in single cells, we narrowed the UV beam to about 5 to 10 μm by inserting a pinhole aperture at the field-stop position of the epi-fluorescence light path of the microscope (*14*). To show that only single cells were activated, we irradiated amnioserosa cells, which do not divide after gastrulation, at the start of gastrulation. Irradiation was restricted to single cells in more than 90% of the attempts; the remainder had two activated cells (Fig. 1C). Photoactivated gene expression did not perturb cellular division or induce cell death. Dorsal epidermis cells, which undergo three rounds of postblastoderm divisions, were irradiated at the start of gastrulation. By stage 13, which is after the normal onset of programmed cell death at stage 12, eight labeled cells could be observed (Fig. 1D).

Mitotic domains are believed to be indicators of cell fate (*15*). DiI labeling has been used to show that cells from mitotic domain 14 give rise to a limited set of neurons (*16*). To test the mitotic domain hypothesis, one must determine the fates adopted by cells of adjacent mitotic domains and show that different mitotic domains produce discrete sets of fates. We compared the fates of cells derived from mitotic domains 2 (∂2), 8 (∂8), and 15 (∂15) (*17*), which are adjacent domains in the anterior ventral region of the embryo (Fig. 2A).

Both single-cell and multiple-cell photoactivation in the head region of ∂2 primarily gave rise to the hypopharyngeal epithelium (floor of the pharynx), macrophages (or hemocytes), and a few cells associated with the pharynx that were provisionally identified as muscle cells. Single-cell activation produced subsets of the multiple-cell activation experiments. The pharyngeal cells often appeared in discrete patterns with associated muscle cells or macrophages (Fig. 2, B and C).

Single-cell irradiation of ∂8 primarily gave rise to endodermal cells that formed the anterior midgut epithelium (Fig. 2D). ∂15 was discerned from ∂8 in that ∂15 cells divide late and abut ∂2. Cells of ∂15 that resided posterior to ∂8 also gave rise to endodermal clones of the anterior midgut epithelium and appeared morphologically similar to ∂8 clones (*12*). It is not clear if cells from both domains intermingle as they migrate from their original location to reside in the endoderm. Irradiation of ∂15 cells that were located lateral to ∂8 stained endodermal cells of the esophagus and proventriculus (Fig. 2E). We have not examined the fates of ∂15 cells that are anterior to ∂8. Clones from both domains often formed clusters and appeared spatially restricted, suggesting a possible targeting mechanism. Whole ∂8 irradiation gave rise to two additional structures, dorsal pharyngeal muscles and visceral muscles of the esophagus and proventriculus. Irradiation of the entire domain labeled mesodermal cells underneath ∂8 because photoactivation of larger areas could not be focused solely to superficial cells and allowed penetration of irradiation to deeper cell layers. We confirmed this result by irradiating ∂10 mesodermal precursors before invagination. Those cells gave rise to the pharyngeal muscles and visceral muscles (*12*).

Fate mapping ∂2, ∂8, and ∂15 showed that there was no fate overlap between ∂2 and ∂15 and limited overlap between ∂15 and ∂8. Clones from ∂8 and ∂15 that contributed to the anterior midgut epithelium could not be discerned by morphology; however, there may be a physiological difference. Also, ∂15 gave rise to clones in the foregut, which were not seen in ∂8. It has been suggested that ∂15 is distinct from ∂8, rather than being a late-dividing component of ∂8, because these cells divide in the plane of the epithelium, not perpendicularly like ∂8. Our results support this conclusion.

It is expected that cells from different regions of the embryo give rise to different

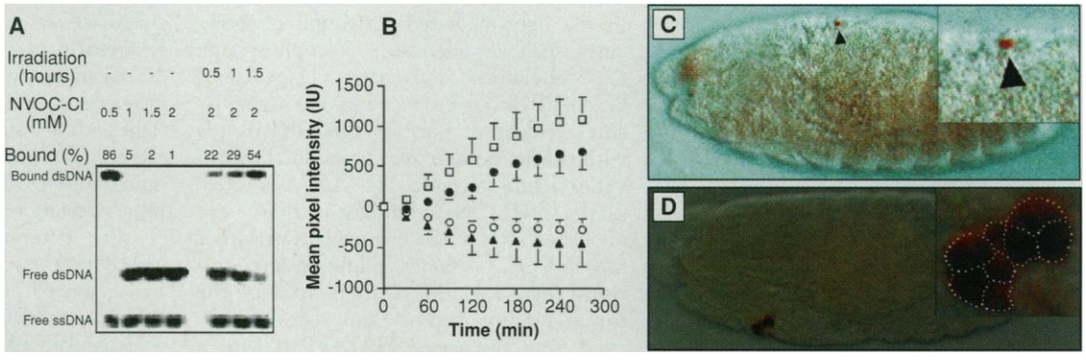

Fig. 1. (**A**) Caging of lysines inhibits DNA binding activity of GAL4VP16, but irradiation partially reverses this inhibition. GAL4VP16 was modified with different concentrations of NVOC-Cl, incubated for 15 min with a radiolabeled, double-stranded (ds), 19-nucleotide DNA containing the GAL4 consensus sequence (*25*), and run on a 16% polyacrylamide gel. Irradiation of the 2 mM samples occurred at 4°C. The percentage of dsDNA bound byGAL4VP16 is shown. Quantitation was done by fluorimaging (Ambis). (**B**) In vivo assay for transcriptional activity of GAL4VP16. Caged or unmodified GAL4VP16 was coinjected with a fluorogenic β-Gal substrate (RGPEG) into embryos of a UAS_G*lacZ* strain, and the changes in whole-embryo fluorescence were recorded by time-lapse recordings with a cooled charge-coupled device (CCD) camera mounted on a fluorescence microscope. The fluorescence intensity units (IU) represent the CCD output values scaled according to the neutral density filter used in recording the image (*26*). Error bars indicate the standard deviation. Within 15 min after injection, embryos injected with caged GAL4VP16 were irradiated with light of a mercury lamp passing through a DAPI (4′,6′-diamidino-2-phenylindole) filter. (□) Average (n = 6) of embryos injected with unmodified GAL4VP16, (●) caged GAL4VP16 irradiated (n = 6), (○) caged GAL4VP16 not irradiated (n = 4), and (▲) RGPEG only (n = 4). (**C**) Immunostain after photoactivation of UAS_G*lacZ* in a single cell of the amnioserosa. Arrowhead points to the labeled cell. Because the level of *lacZ* expression in the amnioserosa was generally weaker than in other tissues, the contrast of the image was enhanced to highlight the stained cell. (Inset) Enlargement of the stained cell. (**D**) Single-cell photoactivation of UAS_G*lacZ* in the dorsal epidermis. The embryo was fixed at stage 13, which occurs after the normal onset of apoptosis. (Inset) Enlargement of the eight-cell cluster with an outline of the individual cells.

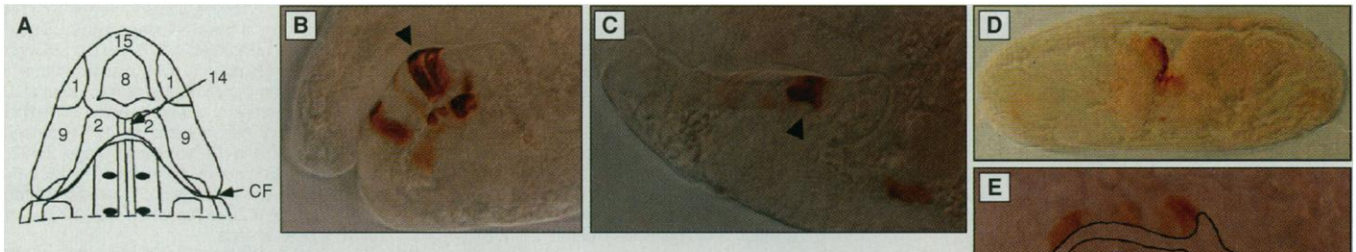

Fig. 2. Cell lineage tracing of cells in domains 2, 8, and 15 after photoactivation of $UAS_G lacZ$. (**A**) Schematic diagram of the ventral mitotic domains in the head primordium. (**B**) ∂2: Single-cell activation labeled cells of the hypopharyngeal epithelium (arrowhead) and associated muscle cells. (**C**) ∂2: Single-cell activation marked the hypopharyngeal epithelium (arrow-head) and macrophages. (**D**) Single-cell activation in ∂8 labeled a cluster of cells in the anterior midgut. (**E**) Activa tion of a single ∂15 cell lateral to ∂8 stained endodermal tissue of the esophagus and proventriculus. The line highlights the lumen of the proventriculus and of the esophagus.

tissues and structures. However, the spatial arrangement of domains ∂2, ∂8, and ∂15 allowed fate mapping of cells that were immediate neighbors on the embryonic surface. It is therefore unlikely that the consistent fate differences from one cell to the next are merely a reflection of the overall location. Thus, the mitotic domain hypothesis is correct: Cells within a particular domain are destined to assume specific fates. Mitotic domain boundaries can therefore be viewed as cell fate boundaries, at least for the mitotic domains described here.

Photoactivated gene expression was also used to induce ectopic expression of a GAL4-dependent *UbxIa* transgene ($UAS_G UBX$).

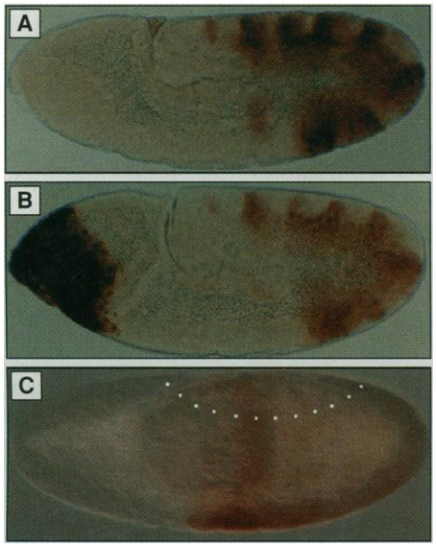

Fig. 3. Immunostains for UBX (**A** and **B**) or ANTP (**C**) after photoactivation of $UAS_G Ubxla$ at the onset of gastrulation. (A) Control. Injection of caged GAL4VP16, no irradiation. (B) Injection of caged GAL4VP16 irradiated anteriorly. (C) $UAS_G Ubxla$ embryo stained for ANTP; unilateral photoactivation of UBX repressed *Antp* transcription only in one-half of the embryo. The approximate area of irradiation is indicated by the dotted line.

Compared to unirradiated embryos (Fig. 3A), the irradiated embryos showed ectopic UBX expression at the site of irradiation (Fig. 3B). Overexpression of UBX in 4- to 7-hour embryos represses *Antennapedia (Antp)* transcription (*18*). Unilateral photoactivation of UBX repressed ANTP expression on one side of the embryo, indicating that the photo-induced UBX was functional (Fig. 3C).

To ectopically activate GAL4-dependent transgenes in *Xenopus*, we injected caged or unmodified GAL4VP16 into *Xenopus* embryos at the four-cell stage together with a reporter plasmid that carried a GAL4-dependent green fluorescent protein (GFP) construct (*19*). Injection of unmodified GAL4VP16 produced high levels of GFP expression (Fig. 4A) that was still visible at stage 31/32. Embryos that were injected with caged GAL4VP16 but not irradiated did not exhibit GFP fluorescence (Fig. 4B); this result was similar to that for embryos that were injected with reporter plasmid alone (*12*). Injection of caged GAL4VP16 followed by irradiation at stage 9 strongly activated expression of GFP, with expression levels comparable to that for unmodified GAL4VP16 (Fig. 4C).

Genetic dissection of development requires both removal and ectopic addition of gene activity. For ectopic gene expression in *Drosophila*, researchers commonly use transgenic heat-shock constructs (*20*) or the GAL4 enhancer trap system (*21*). Also, localized heating of cells with a laser was used to activate the expression of heatshock–responsive transgenes in single cells in *Drosophila* and *Caenorhabditis elegans* (*22*). Photoactivated gene expression complements those two methods in that it extends the window of inducible gene expression to earlier developmental stages and provides a reliable method for spatiotemporal control of ectopic gene expression. The caged GAL4VP16 expression system has the added benefit that localized transient activation of plasmid-borne genes, as was shown in *Xenopus* embryos, may be used in other organisms that are less amenable to genetic manipulation and may increase the throughput of testing different DNA constructs. The main impetus for developing the caged GAL4VP16 photoactivated gene expression system was to provide a method for single-cell fate mapping and ectopic gene expression. Using commercially available reagents and standard biochemical methods as well as standard embryo-preparation techniques, we established a system for light-induced gene expression in *Drosophila* and *Xenopus* embryos. Caged GAL4VP16 can be prepared in a few hours from the purified protein stock and is stable for more than 1 year at −80°C. Typically, we processed about 150 embryos per day.

We have demonstrated that the mitotic domain hypothesis is correct in that mitotic

Fig. 4. Photoactivated gene expression in *Xenopus*. (**A**) Coinjection of unmodified GAL4VP16 and reporter plasmid caused high levels of GFP fluorescence. (**B**) Coinjection of caged GAL4VP16 and reporter plasmid, no irradiation. (**C**) Coinjection of caged GAL4VP16 and reporter plasmid followed by irradiation.

domains are indicators of cell fate. The fates of the cells arising from different mitotic domains had been based on existing fate maps that were generated by visual inspection of unmarked living or fixed embryos. These predictions were confirmed for the domains analyzed thus far. However, direct marking of these cells revealed much more detail about the actual array of fates.

REFERENCES AND NOTES

1. J. H. Kaplan, B. Forbush, J. F. Hoffman, *Biochemistry* **17**, 1929 (1978); G. Marriot and M. Heidecker, *ibid.* **35**, 3170 (1996); S. R. Adams, J. P. Y. Kan, R. Y. Tsien, *J. Am. Chem. Soc.* **111**, 7957 (1989).
2. D. I. Chasman, J. Leatherwood, M. Carey, M. Ptashne, R. D. Kornberg, *Mol. Cell. Biol.* **9**, 4746 (1989). The final preparations were 75 to 80% pure as judged by SDS–polyacrylamide gel electrophoresis. GAL4VP16 was stored at −80°C in storage buffer [50 mM Na-Hepes, 0.2 M NaCl, 1 mM dithiothreitol, 30% glycerol, 0.1 mM EDTA, 10 μM Zn acetate (pH 7.4)].
3. GAL4VP16 was caged according to the following protocol. To one volume of a 1.35 mg/ml solution of the protein in storage buffer (as determined with the Bradford assay) was first added one volume of a 0.1 M sodium carbonate buffer (pH 9.7) and then two volumes of NVOC-Cl (Fluka) in 1,4-dioxane. The pH of the buffer was such that the final pH of the reaction was 9.5. The reaction was carried out for 30 min at room temperature and was stopped by the addition of one volume of acidic 0.1 M tris-HCl, which also lowered the pH to 7.4. GAL4VP16 was found to be very stable under the reaction conditions used. The caged protein was washed twice with Centricon C-30 devices (Amicon) in a 20 mM Na-Hepes, 0.2 M NaCl solution (pH 7.3). The unirradiated, caged GAL4VP16 was stable at −80°C for more than 12 months.
4. The extent of caging was determined by fluorescamine labeling of free amines as described [P. Böhlen, S. Stein, W. Dairman, S. Udenfried, *Arch. Biochem. Biophys.* **155**, 213 (1973)]. Parallel samples of ~30 μg of GAL4VP16 were treated with or without NVOC-Cl according to the standard caging protocol but were washed instead with 50 mM sodium phosphate buffer (pH 8). The samples were then brought to a final volume of 1.5 ml containing 1% SDS and were boiled for 3 min. Fluorescamine (0.5 ml, 30 mg/100 ml; Molecular Probes) in 1,4-dioxane was added, and the fluorescence of the sample was analyzed with a fluorimeter (excitation at 390 nm, emission at 485 nm). Results of the caged protein samples were correlated with that of the control sample that was incubated without NVOC-Cl.
5. Embryos were prepared for injection as described [J. S. Minden, D. A. Agard, J. W. Sedat, B. M. Alberts, *J. Cell Biol.* **109**, 505 (1989)]. All injections were done during interphase 14. For immunostaining, embryos were fixed and manually devitellinized as described [J. P. Vincent and J. P. O'Farrell, *Cell* **68**, 923 (1992)]. After devitellinization, embryos were washed briefly in methanol (30 s), and antibody staining was carried out by standard protocols as reported [H. M. Bomze and A. J. Lopez, *Genetics* **136**, 965 (1994)]. 5C.2B (anti-UBX) was diluted 1:65, 4CI-I (anti-ANTP) was diluted 1:33, anti-GAL4 (Santa Cruz Biotechnology) was diluted 1:1000, and anti–β-Gal (Sigma) was diluted 1:1500.
6. Presumably, this level of modification inhibited GAL4VP16 binding to chromatin, rather than naked DNA, or interfered with specific protein-protein interactions. Anti-GAL4 staining showed that caging did not perturb nuclear localization (*12*).
7. Ultraviolet doses for photoactivation were quantitated by actinometry as described [C. G. Hatchard and C. A. Parker, *Proc. R. Soc. London.* **A235**, 518 (1956)] with an assumed quantum yield of 1.26 at 366 nm. *Drosophila* photoactivations were done with a UPlanFl 60×/1.25 oil-immersion objective on an Olympus IX-70 microscope with an Olympus IX-RFA/Caged attachment. The beam used for photoactivation of single mitotic cells in *Drosophila* embryos delivered an energy dose of about 8 μJ per second. Thus, a total of 24 μJ were necessary for photoactivation of a single cell. Photoactivation of entire *Xenopus* embryos required about 82-fold as much energy per area than individual *Drosophila* cells. In vitro photoactivation with the hand-held UV lamp was less efficient than in the in vivo experiments by a factor of about 8200, which explains the long irradiation times necessary for the gel mobility-shift assay.
8. J. S. Minden, *Biotechniques* **20**, 122 (1996).
9. Concentrations of injected GAL4VP16 were adjusted to the dryness of the embryo preparation and to the site of injection. If the injection occurred close to the anterior tip, the concentration was decreased by as much as 80% because of the limited diffusion at the poles.
10. G. Gill and M. Ptashne, *Nature* **334**, 721 (1988).
11. G. B. Afanas'eva, T. S. Viktorova, K. I. Pashkevich, I. Y. Postovskii, *Chem. Heterocyclic Comp.* **10**, 302 (1974).
12. S. B. Cambridge and J. S. Minden, data not shown.
13. J. M. Abrams, K. White, L. I. Fessler, H. Steller, *Development* **117**, 29 (1993); R. Namba, T. M. Pazdera, R. L. Cerrone, J. S. Minden, *ibid.* **124**, 1393 (1997).
14. A 400-μm pinhole was used for single-cell irradiation in the amnioserosa tissue and a 600-μm pinhole was used for single mitotic cells.
15. V. E. Foe, *Development* **107**, 1 (1989).
16. T. Bossing and G. M. Technau, *ibid.* **120**, 1895 (1994).
17. Mitotic domains were identified by differential interference contrast microscopy of mitotic cells, which swell up and protrude above the nondividing epithelium. Alternatively, mitotic domains were visualized by fluorescence confocal microscopy of a transgenic strain that constitutively expressed a nuclear-localized GFP (*23*). The different mitotic domains were identified by the time of appearance, the location, and the shape of the mitotic patch. ∂2 is a golf club–shaped group of cells that form immediately anterior to the cephalic furrow, with the head of the golf club at the ventral midline and the shaft oriented parallel to the cephalic furrow. ∂8 forms a circular cluster of cells that straddle the ventral midline anterior to ∂2. ∂8 is completely surrounded by ∂15, which forms a single row of cells separating ∂8 from ∂2, ∂9, ∂1, and ∂23. Stained tissues were identified on the basis of their morphology, location, and embryonic origin (*24*).
18. A. Gonzáles-Reyes and G. Morata, *Cell* **61**, 515 (1990).
19. Albino *Xenopus* embryos were injected with 5 nl into each blastomere at the 4-cell stage with 0.05 mg/ml caged or unmodified GAL4VP16 and 0.0125 mg/ml $UAS_G GFP$ (S65T) plasmid (GFP was fused to a nuclear localization signal). Embryos were kept at 19° to 20°C at all times and were injected superficially into the animal hemisphere. At 19°C, embryos reached stage 9 in 12 hours and stage 31/32 in about 2 days. Embryos were irradiated for 45 to 60 s with UV light from a standard UV filter set (Chroma Technology) on a Zeiss Axiophot, with the use of a 10×/0.5 Fluar air-lens.
20. J. T. Lis, J. A. Simon, C. A. Sutton, *Cell* **35**, 403 (1983).
21. A. H. Brand and N. Perrimon, *Development* **118**, 401 (1993).
22. J. Harris, L. Honigberg, N. Robinson, C. Kenyon, *ibid.* **122**, 3117 (1996); E. G. Strigham and E. P. M. Candido, *J. Exp. Zool.* **266**, 227 (1993); M. S. Halfon, H. Kose, A. Chiba, H. Keshishian, *Proc. Natl. Acad. Sci. U.S.A.* **94**, 6255 (1997).
23. I. Davis, C. H. Girdham, P. H. O'Farrell, *Dev. Biol.* **170**, 726 (1995).
24. G. M. Technau and J. A. Campos-Ortega, *Roux's Arch. Dev. Biol.* **194**, 196 (1985).
25. E. Gininger, S. Varnum, M. Ptashne, *Cell* **40**, 767 (1985).
26. The fluorescence intensity units plotted are corrected for background fluorescence. For each time point, the fluorescence value at $t = 0$ of the respective curve was subtracted. The original uncorrected fluorescence units at $t = 0$ were 975 (□), 949 (●), 857 (○), and 1078 (▲).

27. We thank V. Hartenstein for help with the identification of the stained tissues and J. Ambroziak for help with the gel mobility-shift assays. The $UAS_G lacZ$ stock was provided by N. Perriman. The $UAS_G Ubxla$ stock and anti-UBX antibody was provided by J. Lopez. We thank B. Schmidt and members of the reagent group at the Science and Technology Center for Light Microscope Imaging and Biotechnology for helpful comments and W. McClure, J. Lopez, D. L. Taylor, A. Koretsky, and members of the Minden lab for critical review of the manuscript. Supported by a NSF Training Grant Fellowship, a Lucille Markey Charitable Trust Interdisciplinary Program in Biotechnology Fellowship, and the Friedrich-Naumann-Stiftung (S.B.C.) and by the Medical Foundation (Fleet Bank Trustee) (R.L.D.) and NSF Center for Light Microscope Imaging and Biotechnology grant BIR-8920118 (J.S.M.). J.S.M. is a Lucille Markey Scholar. This work was supported in part by a grant from the Lucille P. Markey Charitable Trust.

6 March 1997; accepted 27 June 1997

The Influence of Dominance Rank on the Reproductive Success of Female Chimpanzees

Anne Pusey,* Jennifer Williams, Jane Goodall

Female chimpanzees often forage alone and do not display obvious linear dominance hierarchies; consequently, it has been suggested that dominance is not of great importance to them. However, with the use of data from a 35-year field study of chimpanzees, high-ranking females were shown to have significantly higher infant survival, faster maturing daughters, and more rapid production of young. Given the foraging behavior of chimpanzees, high rank probably influences reproductive success by helping females establish and maintain access to good foraging areas rather than by sparing them stress from aggression.

In many species of group-living mammals, especially those that feed on monopolizable foods, such as spotted hyenas and many primates, females have frequent dominance interactions and are ranked in stable linear hierarchies (*1–4*). These hierarchies result from, and are maintained by, a pattern of alliances in which close relatives support each other against more distant relatives and high-ranking matrilines support each